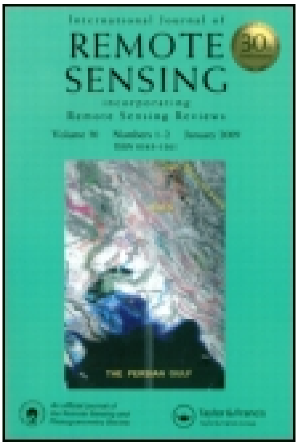

International Journal of Remote Sensing
Publication details, including instructions for authors and subscription information:
http://www.tandfonline.com/loi/tres20

Validation of MODIS, MISR, OMI, and CALIPSO aerosol optical thickness using ground-based sunphotometers in Hong Kong

Man Sing Wong [a], Muhammad I. Shahzad [a], Janet E. Nichol [a], Kwon Ho Lee [b] & P.W. Chan [c]

[a] Department of Land Surveying and Geo-Informatics, The Hong Kong Polytechnic University, Kowloon, Hong Kong

[b] Department of Satellite Geoinformatics Engineering, Kyungil University, Geongsan, 712-701, Republic of Korea

[c] Hong Kong Observatory, Hong Kong

Version of record first published: 02 Oct 2012.

To cite this article: Man Sing Wong, Muhammad I. Shahzad, Janet E. Nichol, Kwon Ho Lee & P.W. Chan (2013): Validation of MODIS, MISR, OMI, and CALIPSO aerosol optical thickness using ground-based sunphotometers in Hong Kong, International Journal of Remote Sensing, 34:3, 897-918

To link to this article: http://dx.doi.org/10.1080/01431161.2012.720739

International Journal of Remote Sensing
Vol. 34, No. 3, 10 February 2013, 897–918

Validation of MODIS, MISR, OMI, and CALIPSO aerosol optical thickness using ground-based sunphotometers in Hong Kong

Man Sing Wong[a], Muhammad I. Shahzad[a], Janet E. Nichol[a]*, Kwon Ho Lee[b], and P.W. Chan[c]

[a]*Department of Land Surveying and Geo-Informatics, The Hong Kong Polytechnic University, Kowloon, Hong Kong;* [b]*Department of Satellite Geoinformatics Engineering, Kyungil University, Geongsan 712-701, Republic of Korea;* [c]*Hong Kong Observatory, Hong Kong*

(*Received 12 January 2012; accepted 18 July 2012*)

Aerosol observations are essential for understanding the Earth's radiation budget and the complexities of climate change, as they are involved in the backscattering of solar radiation and the formation of cloud condensation nuclei. In Hong Kong, the most direct effect is on air quality. Atmospheric haze caused by the emission of aerosols from industrial and vehicular sources creates visibility lower than 8 km for approximately 20% of the time, having risen at 6% per decade since 1980, but regional emissions are at least as influential as local ones. The 179,000 km^2 covered by Hong Kong and neighbouring Guangdong Province cannot be adequately covered by the 76 monitoring stations set up by the two governments, and satellite images offer the only potential source of regional air quality data. However, the current satellite-based aerosol optical thickness (AOT) products are intended for global air quality monitoring, and may contain errors over a humid coastal city such as Hong Kong and its surrounding industrialized regions. This research compares the AOT retrieved from several AOT operational products, namely the Moderate Resolution Imaging Spectroradiometer (MODIS) MOD04 product, the MODIS 500 m product, the Multiangle Imaging Spectroradiometer (MISR) product, the Ozone Monitoring Instrument (OMI) multiwavelength aerosol product, and the Cloud-Aerosol Lidar and Infrared Pathfinder Satellite Observation (CALIPSO) product, with ground-based AOT from sunphotometers in Hong Kong. These sunphotometers include two AERONET stations, and are deployed in Hong Kong over urban, suburban, and coastal areas. The rigorous correlations, root mean square errors, and mean absolute differences available from the multilocational field data within one city region provide a strong base for validating the AOT products from different sensors and at different spatial scales over different land surface types. The results suggest that the AOT products, especially those from MODIS 10 km, provide reliable and accurate observations for daily air quality monitoring over a variety of land-cover types, as well as for identifying emission sources for coordinated actions by the governments of Hong Kong and the Chinese mainland.

1. Introduction

Aerosols are defined as particles suspended in the atmosphere in either liquid or solid form. They have different size distributions, shapes, and residence times, and are from different sources. The study of aerosols is important because of their effects on the Earth's radiation

*Corresponding author. Email: lsjanet@inet.polyu.edu.hk; lsjanet@polyu.edu.hk

ISSN 0143-1161 print/ISSN 1366-5901 online

http://dx.doi.org/10.1080/01431161.2012.720739
http://www.tandfonline.com

budget, climate change, atmospheric conditions, and human health. Recent research has focused on fine aerosols for their long-term damage to the respiratory system (Davidson, Phalen, and Solomon 2005; Dominici et al. 2006). At the global level, aerosols, and the clouds that are closely associated with them, play an especially important role in the Earth's energy budget. Aerosols, which serve as condensation nuclei, are key elements in cloud formation. Traditionally, aerosols are considered to be equivalent to 'haze' and 'dust'. Early observations of aerosols were carried out visually. In the last hundred years, there have been many observations and studies of aerosols. Mie (1908) developed a theory for analysing aerosol particle sizes and their optical characteristic, hence the term 'Mie particles'. Junge (1952) first illustrated the continuous aerosol size distribution, covering radii from 0.01 to 10 μm, where particles less than 0.1 μm are produced by reactive gases in the atmosphere such as sulphur dioxide (SO_2) or fires, and particles larger than 1 μm are produced by natural environmental processes such as from wind-blown soil and sea salt (Hobbs 1993).

Multichannel algorithms for retrieving aerosol optical thickness (AOT) from satellite data have been devised over the last three decades, and they are now potentially able to address the shortcomings of air particulate measurements at a few ground stations covering a region, because satellites provide large spatial coverage whereas ground stations only represent their neighbouring regions and cannot be used for locating emission sources. Different algorithms have been developed for aerosol retrieval over (1) water (Martonchik et al. 1998; Kaufman and Tanré 1998; Kahn, Banerjee, and McDonald, 2001; Remer et al. 2002), (2) vegetation (Kaufman and Sendra 1988; Kaufman et al. 1997), (3) bright surfaces such as deserts (Martonchik et al. 1998; Kaufman et al. 2002; Hsu et al. 2004; Kahn et al. 2005; Hsu, Tsay, and King 2006; Kokhanovsky et al. 2007), and (4) complex surfaces such as urban areas (Kahn et al. 2005; Lee et al. 2006; Von Hoyningen-Huene et al. 2006; Kokhanovsky et al. 2007; Lee and Kim 2010; Wong et al. 2010; Wong, Nichol, and Lee 2011). The need for different algorithms is due to the different wavelengths used by different sensors (Hidy et al. 2009). The general rationale of multiwavelength aerosol retrieval is to separate the atmospheric contribution and surface reflectance from the total image signal at the top-of-atmosphere (TOA). However, a decade of research on algorithms for multiwavelength aerosol retrieval has not achieved very high accuracy, especially for retrievals over complex land surfaces such as urban and urbanized regions (King et al. 1999; Lee et al. 2009). Additionally, the south China region including Hong Kong was originally identified as an area with a particularly large error of satellite-derived estimates of AOT (Kaufman and Tanré 1998), due to its unique high AOT, mixed particulate types, high humidity, high cloud cover, and turbid coastal waters, and this has not yet been addressed.

The Moderate Resolution Imaging Spectroradiometer (MODIS) is a sensor on board the TERRA and AQUA satellites (Parkinson 2003). TERRA was launched in 1999 and passes from north to south in the morning (∼10:30 a.m. local time at equator) and AQUA was launched in 2001 and passes from south to north in the afternoon (∼1:30 p.m. local time at equator). With 36 wavebands at 250 m, 500 m, and 1 km resolution, MODIS can be used for atmospheric, oceanic, and land studies at both global and local scales. Currently, the MODIS level 2 operational aerosol product (MOD04) provides 10 km resolution AOT values and has been upgraded from collection 4 (Kaufman et al. 1997; Kaufman and Tanré 1998) to collection 5 (Levy et al. 2005; Remer et al. 2005), with more consideration of aerosol types and dark pixel selection during retrieval. The rationale of the multiwavelength algorithm used in MODIS is to take advantage of different aerosol scattering properties (e.g. longer wavelengths have smaller aerosol loadings). Thus, by virtue of their spectral differences, the amount of aerosol reflectance can be inferred from a combination of longer and shorter wavelengths. The derived aerosol reflectances are then fitted to look-up tables

(LUTs) created from different aerosol types to derive AOT. However, since the current operational product does not work adequately over complex surfaces such as urbanized regions and at higher resolution, a new method using the minimum reflectance technique (MRT) was developed (Wong et al. 2010; Wong, Nichol, and Lee 2011) to provide an AOT product at 500 m from MODIS. This permits mapping of AOT over Hong Kong and the Pearl River Delta (PRD) region at a more detailed level.

The Multiangle Imaging Spectroradiometer (MISR) was launched in 1999 as a polar orbiting sun-synchronous satellite (TERRA) at an altitude of 705 km, with temporal resolution of 16 days. MISR has nine cameras with four spectral bands (446, 558, 672, and 867 nm), which are used for observing forward, nadir, and rear from nine different viewing angles (Diner et al. 1998). The nominal spatial resolutions of MISR are 250 m, 275 m, and 1 km, but radiances at 1.1 km resolution are processed to give the standard level-2 MISR aerosol product at a 17.6 km $\times$ 17.6 km pixel size. The heterogeneous land algorithm was developed by Martonchik et al. (1998) for application with multiple viewing angle sensors when no dense dark vegetation (DDV) but sufficient spatial contrasts are present in a scene. It differs from the dark water and DDV retrieval methods, and uses the spatial contrasts between pixels to derive an empirical orthogonal function (EOF) based on different angular variations of the image reflectance. The path reflectance can be determined from these differences. The resulting AOT values can be devised from the best-fitting aerosol model (Martonchik et al. 1998; Diner et al. 1998).

The Ozone Monitoring Instrument (OMI) was launched in 2004 on a 705 km sun-synchronous polar orbit on the AURA satellite with an ascending node equator crossing time of 1:45 p.m. (LST) (Dobber et al. 2006; Levelt et al. 2006). The OMI instrument with advance viewing capabilities is an inheritor of instruments such as the Total Ozone Mapping Spectrometer (TOMS) (Heath and Park 1978; Bhartia and Wellemeyer 2002), the Solar Backscatter Ultraviolet Instrument (SBUV) (Heath and Park 1978), the Global Ozone Monitoring Instrument (GOME) (Burrows et al. 1999), and the Scanning Imaging Absorption Spectrometer for Atmospheric Cartography (SCIAMACHY) (Burrows et al. 1995; Bovensmann et al. 1999). The OMI instrument is a push-broom, nadir-viewing, ultraviolet–visible (ultraviolet: 270–365 nm and visible: 365–500 nm) imaging spectrometer with a wide instantaneous across-track field of view (115°). These wavelength ranges are used to retrieve the OMI data products, which are available at four processing levels (level 0, level 1B, level 2, and level 3). The OMI operational algorithms to retrieve these data products depend heavily on experience gained from TOMS, GOME, SBUV, and SCIAMAMCHY. There are two aerosol products developed for OMI: the OMAERUV aerosol product (near-UV algorithm) and OMAERO aerosol product (multiwavelength algorithm). The near-UV algorithm derives AOT from the 342.5 and 388 nm wavelengths. Its rationale is to first derive the aerosol index from these two wavelengths, then to use the aerosol index to determine the best-fitting aerosol type. Lastly, it uses the best-fitting aerosol type to generate an LUT, which is used to derive AOT and the single scattering albedo (SSA). The multiwavelength algorithm derives AOT using eight UV and visible wavelengths from 340 to 500 nm. Its rationale is to fit the spectrum to 50 aerosol models, and find the model with the least systemic error (least root mean square error (RMSE)), and then further derive the AOT value from the appropriate aerosol model (Torres et al. 2005). In this study, the OMAERO aerosol grid product from the multiwavelength algorithm (at 27.8 km spatial resolution) was used since it provides AOT values at visible wavelengths that are compatible with sunphotometer measurements.

The CALIPSO (Cloud-Aerosol Lidar and Infrared Pathfinder Satellite Observation) spacecraft was launched in 2006 to observe the vertical structure and properties of clouds and aerosols (Winker, Pelon, and Mccormick 2003; Winker, Hunt, and Mcgill 2007; Winker et al. 2010). CALIPSO is the first satellite-borne polarization lidar. It is placed in a 705 km sun-synchronous polar orbit, providing global coverage between 82 °N and 82 °S with a local afternoon equatorial crossing time of 1:30 p.m. (ascending node). The CALIPSO payload consists of CALIOP (Cloud-Aerosol Lidar with Orthogonal Polarization), an active and polarization-sensitive lidar instrument with passive visible and infrared sensors (Winker, Pelon, and Mccormick 2003). The main objective of CALIPSO is to provide high-resolution vertical profiles and spatial and optical properties of aerosols and clouds to improve understanding of the global climate and for weather forecasting and air quality models (Winker, Hunt, and Mcgill 2007). The accuracy of CALIOP data products depend on the calibration of the 532 nm backscatter profiles, which are divided into level 1 and level 2 (King et al. 2004). The level 1 data products consist of geo-located and calibrated profiles. The level 2 data products have three types of data: layer products (properties of clouds and aerosol layers), profile products (backscatter and extinction profiles), and a vertical feature mask (location and types of aerosols and clouds). The column AOT from level 2 products with a spatial resolution of 5 km is used in this study.

This research aims to compare and validate the AOT products from five satellite sensors (MODIS 10 km, MODIS 500 m, MISR, OMI, and CALIPSO) with AOT measured by three sunphotometers in Hong Kong. The three sunphotometers include two AERONET stations, allowing AOT data to be collected over urban areas, suburban areas, and coastal areas. This may be the second densest sunphotometer campaign in the world, as three sunphotometers are deployed over an area of 1104 km^2 in this study, while the densest campaign is the DRAGON-US experiment operated by NASA in 2011 (DRAGON-US 2011). The results from the evaluation can suggest the best parameters for reliable and accurate daily air quality monitoring over an urbanized region and also for identifying emission sources for coordinated actions by the governments of Hong Kong and the Chinese mainland.

2. Study area and data used

The skies over Hong Kong are obscured for 20% of the time during the year due to frequent episodes of reduced visibility (visibility less than 8 km) (Chang and Koo 1986; Lai and Sequeira 2001). These low visibilities are thought to be due to interactions between anthropogenic aerosols, sea salts, water vapour, and long-distance dust (Bell, Peterson, and Chin 1970). In addition, a significant 22% increase in AOT has occurred between 2002 and 2004 (Cheng, Chan, and Yang 2006). During the dry season, northerly and northeasterly winds bring continental pollution from industries in the neighbouring PRD region of the Chinese mainland to Hong Kong. The PRD region is deemed to be the main source of anthropogenic emissions in south China.

This study used satellite data for many years from several different sensors, namely (1) the MODIS 10 km AOT product at 550 nm from years 2000 to 2010, (2) the MODIS 500 m AOT product at 550 nm (Wong et al. 2010; Wong, Nichol, and Lee 2011) from years 2000 to 2011, (3) the MISR 17.6 km AOT product at 446, 558, 672, and 866 nm from years 2005 to 2010, (4) the OMI 27.8 km AOT product at 342, 388, 442, 463, and 483 nm from years 2004 to 2010, and (5) the CALIPSO 5 km AOT product at 532 and 1064 nm from years 2006 to 2010. The AOT products derived from these satellites were validated using three sunphotometers. Two of these, an urban site (Hong Kong PolyU) and a rural coastal site (Hong Kong Hok Tsui), belong to the AERONET network. AERONET is a federated network of ground sunphotometers, which measure the aerosol extinction every 15 min over multiple wavelengths (Holben et al. 1998). The Hong Kong PolyU urban site, situated

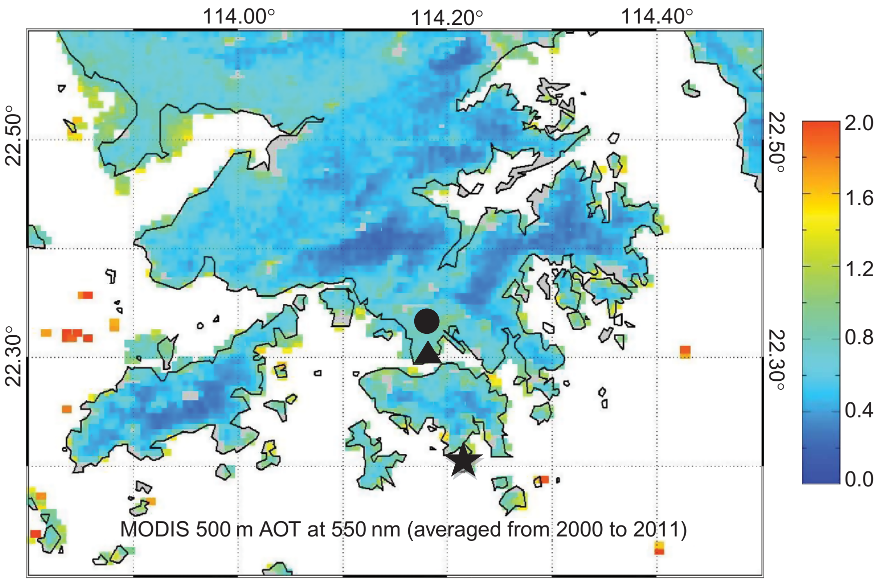

Figure 1. Aerosol monitoring stations in Hong Kong overlaid onto a MODIS 500 m AOT image (average of AOT from 2000 to 2011). The triangle represents Hong Kong PolyU AERONET station, the star represents Hong Kong Hok Tsui AERONET station, and the circle represents Hong Kong CityU sunphotometer.

at the centre of the urbanized Kowloon Peninsula (Figure 1), has operated since 2005, and the Hong Kong Hok Tsui rural site, located on a remote peninsula near the coast, was set up to monitor rural (background) aerosols and has operated from 2007 to 2010. A third, standalone sunphotometer was operated at a suburban location at the City University of Hong Kong from 2002 to 2009.

3. Methodology

Validation of MODIS 10 km, MODIS 500 m, MISR, OMI, and CALIPSO AOT products in Hong Kong was undertaken by comparison with the two AERONET level 1.5 data and data from one standalone sunphotometer. The AERONET level 1.5 data are cloud-screened by a NASA operational algorithm (Smirnov et al. 2000). For this, the MODIS 10 km, MODIS 500 m, MISR, and CALIPSO products were compared with AERONET and sunphotometer observations within a period of ±30 min of overpass time (Ichoku et al. 2002). The OMI grid products were compared with daily AERONET and sunphotometer observations. The columnar AOTs were then extracted from a 3 by 3 kernel for image pixels corresponding to the three ground sunphotometer stations, for MODIS 10 km, MODIS 500 m, MISR, and OMI products. However, since CALIPSO has a much lower visit frequency over Hong Kong, a larger kernel with 8×8 pixels was used.

4. Results

4.1. MODIS AOT versus sunphotometer AOT data

The MODIS 10 km AOT was found to be highly correlated with the PolyU AERONET, Hok Tsui AERONET, and CityU AOT (correlation (r) = 0.950, 0.944, and 0.945, respectively)

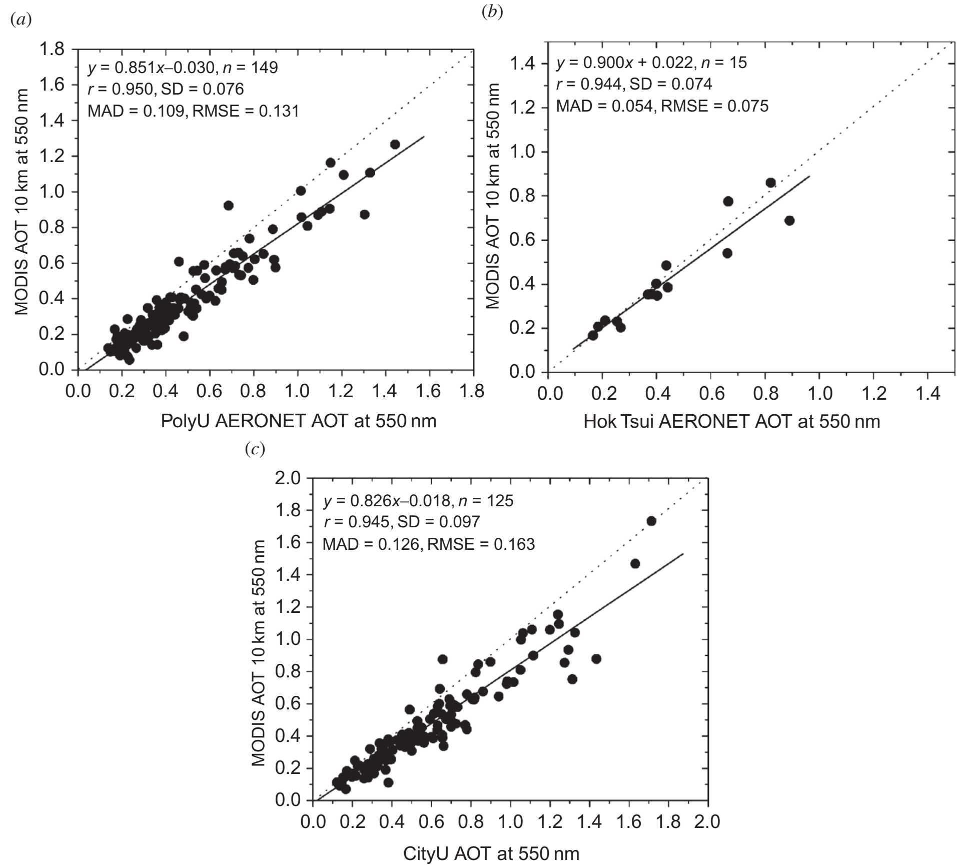

Figure 2. Comparison between the MODIS 10 km product and (*a*) Hong Kong PolyU AERONET data, (*b*) Hong Kong Hok Tsui AERONET data, and (*c*) CityU sunphotometer data, all at 550 nm.

(Figure 2). Approximately three-quarters of the data fall within ±0.1 of the AERONET AOT values, and the mean absolute differences (MADs) and RMSEs between AOTs and sunphotometer data are 0.109, 0.054, and 0.126, and 0.131, 0.075, and 0.163 for PolyU, Hok Tsui, and CityU sunphotometer measurements, respectively. This performs better than the MODIS 500 m AOT ($r = 0.872$, 0.931, and 0.856). The MADs are 0.100, 0.122, and 0.129, and the RMSEs are 0.118, 0.135, and 0.160 for PolyU, Hok Tsui, and CityU, respectively (Figure 3). The reason for only moderate performance observed for the MODIS 500 m AOT is thought to be mainly due to the estimation of surface reflectance (Wong et al. 2010; Wong, Nichol, and Lee 2011).

4.2. MISR AOT versus sunphotometer AOT data

The MISR 17.6 km AOT product in general shows high correlations with ground-based sunphotometers, except for those at the coastal Hok Tsui AERONET site. The correlations between the MISR product and the PolyU AERONET are $r = 0.914$, 0.908, 0.890, and 0.873 at 446, 558, 672, and 886 nm, respectively. Similar high correlations were also observed for the CityU sunphotometer site, where $r = 0.875$, 0.880, 0.824, and 0.692 were

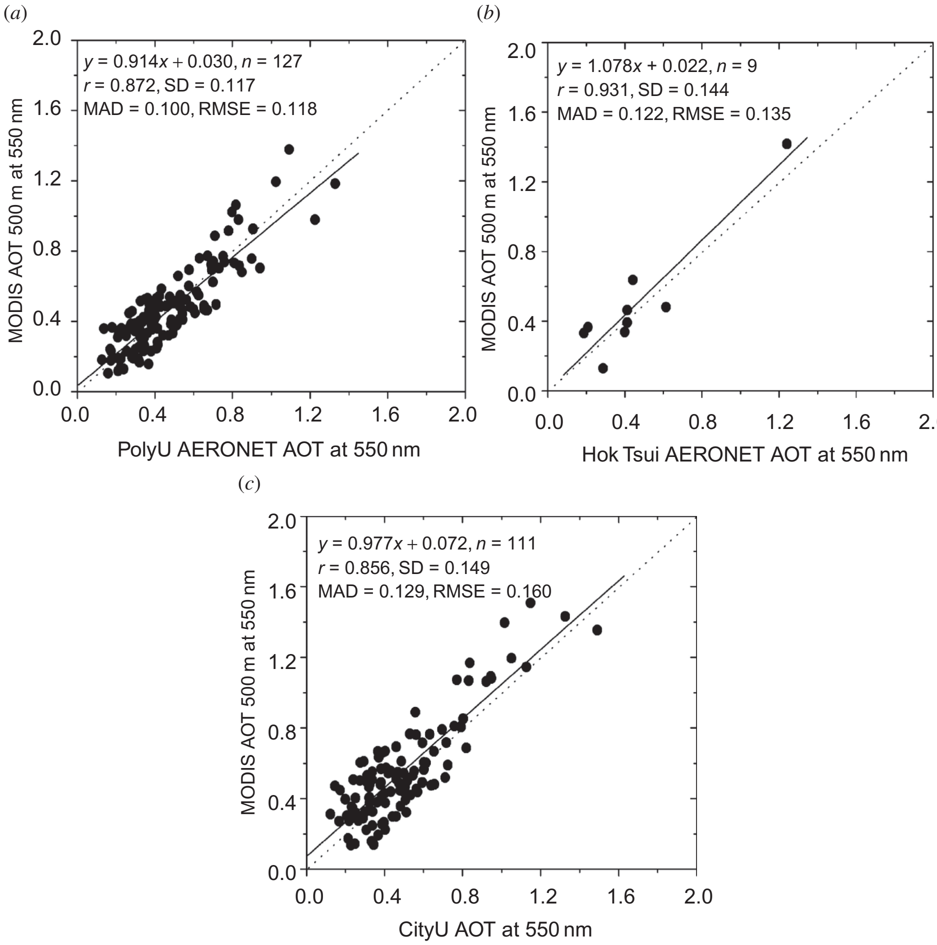

Figure 3. Comparison between the MODIS 500 m product and (*a*) Hong Kong PolyU AERONET data, (*b*) Hong Kong Hok Tsui AERONET data, and (*c*) CityU sunphotometer data, all at 550 nm.

observed at 446, 558, 672, and 886 nm, respectively (Figure 4). Although fewer suitable images were obtained due to the lower visit frequency of MISR than MODIS, these sampling numbers are still statistically significant at the 1% interval (e.g. the observed correlation of 20 samples should exceed the correlation (r) of 0.733 to be significant at the 1% confidence interval) except 886 nm at CityU comparison. The Hok Tsui site has operated only since 2007 and there are not enough matched data for comparison. Lower MADs and RMSEs are obtained from the PolyU site (0.179 and 0.217 at 550 nm) compared with CityU (0.232 and 0.303 at 550 nm). The high correlations observed over urban and suburban areas are in line with the findings reported by Liu et al. (2010) and Jiang et al. (2007) in China. MISR AOT showed good correlation with the ground data, which may be because a large number of aerosol models, incorporating aerosol mixtures from different aerosol parameters including shape, size, and mass, are considered in the MISR AOT retrieval algorithm (Martonchik et al. 1998; Kahn, Banerjee, and Mcdonald 2001). However, this approach may also be a drawback as the aerosol models are derived from research conducted for specific regions and thus may not be applicable globally.

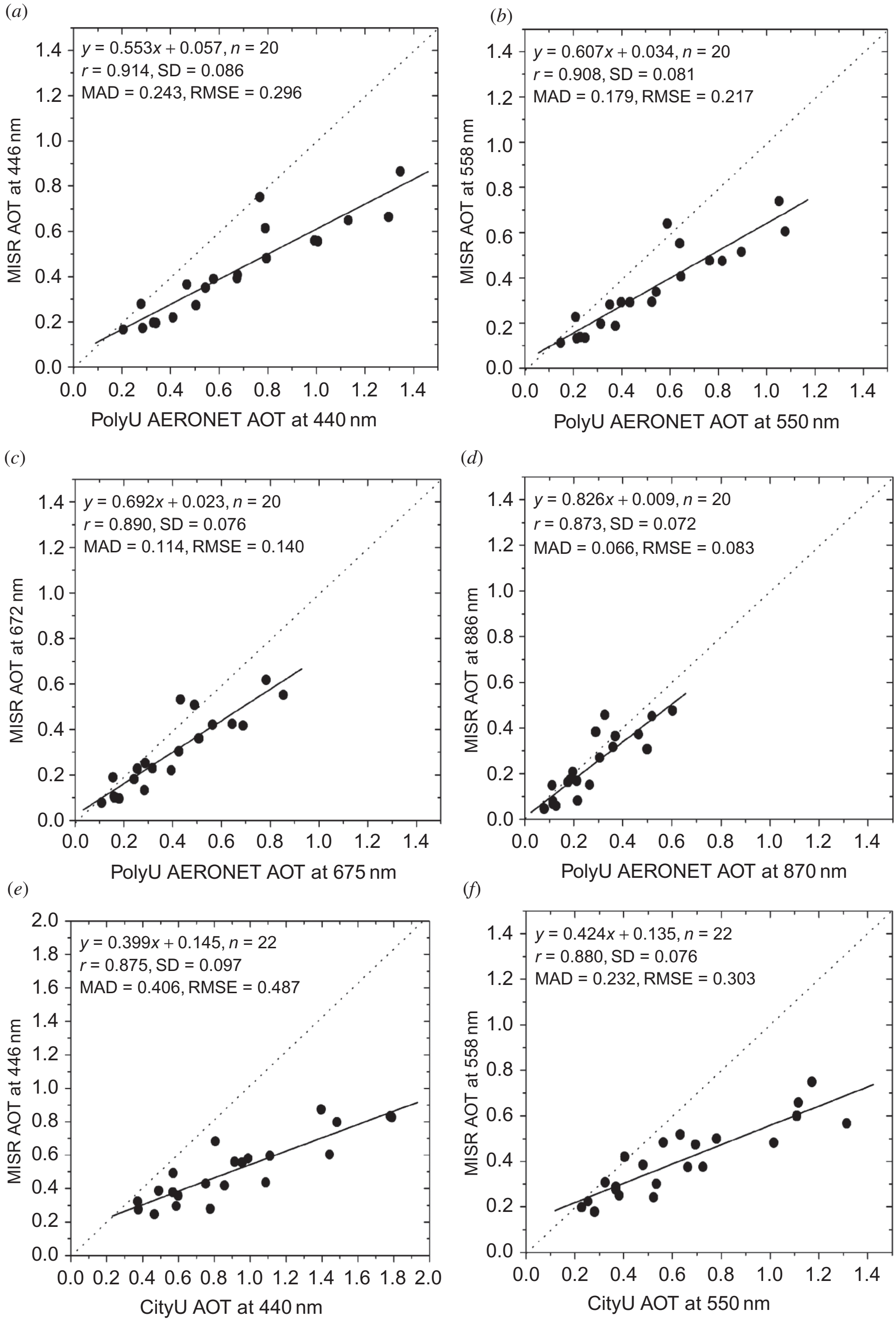

Figure 4. Comparison between the MISR 17.6 km product and Hong Kong PolyU AERONET data at (*a*) 440 nm, (*b*) 550 nm, (*c*) 675 nm, and (*d*) 870 nm, and CityU sunphotometer data at (*e*) 440 nm, (*f*) 550 nm, (*g*) 675 nm, and (*h*) 870 nm.

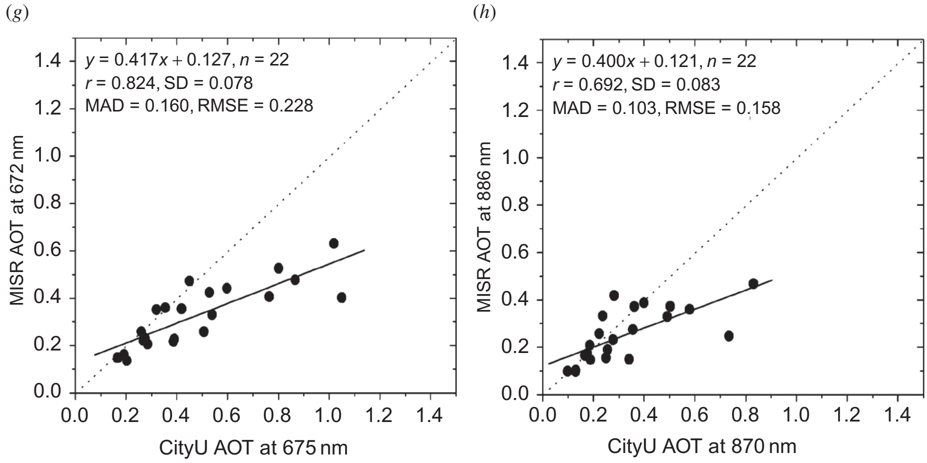

Figure 4. (*Continued*).

4.3. OMI AOT versus sunphotometer AOT data

Figure 5 shows the correlation between the AOT retrieved from OMI and AERONET at five different wavelengths. The correlation between the OMI product and PolyU AERONET is $r = 0.570$, which is higher than that for the Hok Tsui AERONET ($r = 0.490$) but lower than that for the CityU sunphotometer ($r = 0.707$). Lower MADs and RMSEs are also found for CityU (averaged values of MADs and RMSEs are 0.259 and 0.359, respectively) than for PolyU (0.432 and 0.615) and Hok Tsui (0.497 and 0.705) AERONET sites. In general, the OMI product overestimates AOT, which may be due to subpixel cloud contamination since the large pixels can easily contain undetected cloud. This overestimation supports the arguments of Curier et al. (2008), which indicate the limitations of the OMI in mapping AOT over a coastal region due to unreliable values of surface albedo in the presence of mixed pixels. In addition, Torres et al. (1998) and Jethva and Torres (2011) found that the discrepancy in OMI-retrieved AOT is caused by the underestimation of the assumed aerosol layer height. Uncertainty in the retrieval of AOT from OMI is normally associated with subpixel cloud contamination, assumed aerosol layer height, surface albedo effect, and error contributed by the assumed aerosol model.

4.4. CALIPSO AOT versus sunphotometer AOT data

The main objective of CALIPSO is to measure the aerosol vertical profile from space-borne lidar. The summarization of the extinction coefficient at different altitudes is deemed to be equal to AOT. Low correlations were observed between CALIPSO and ground-based sunphotometer data, e.g. PolyU AERONET site ($r = 0.275$ and 0.021 at 532 and 1064 nm, respectively) and CityU site ($r = 0.225$ and 0.184 at 532 and 1064 nm, respectively) (Figure 6). The insufficient number of data pairs, e.g. sample numbers of 17 and 5, cannot be counted as statistically significant. The low correlation may be due to the limitation of CALIPSO in collecting data from near ground level during the daytime, with a lower signal-to-noise ratio expected due to the high solar background (Hidy et al. 2009).

The AOT images of MODIS 10 km, MODIS 500 m, MISR, OMI, and CALIPSO over Hong Kong are shown in Figure 7, and the averaged AOT images are shown in Figure 8.

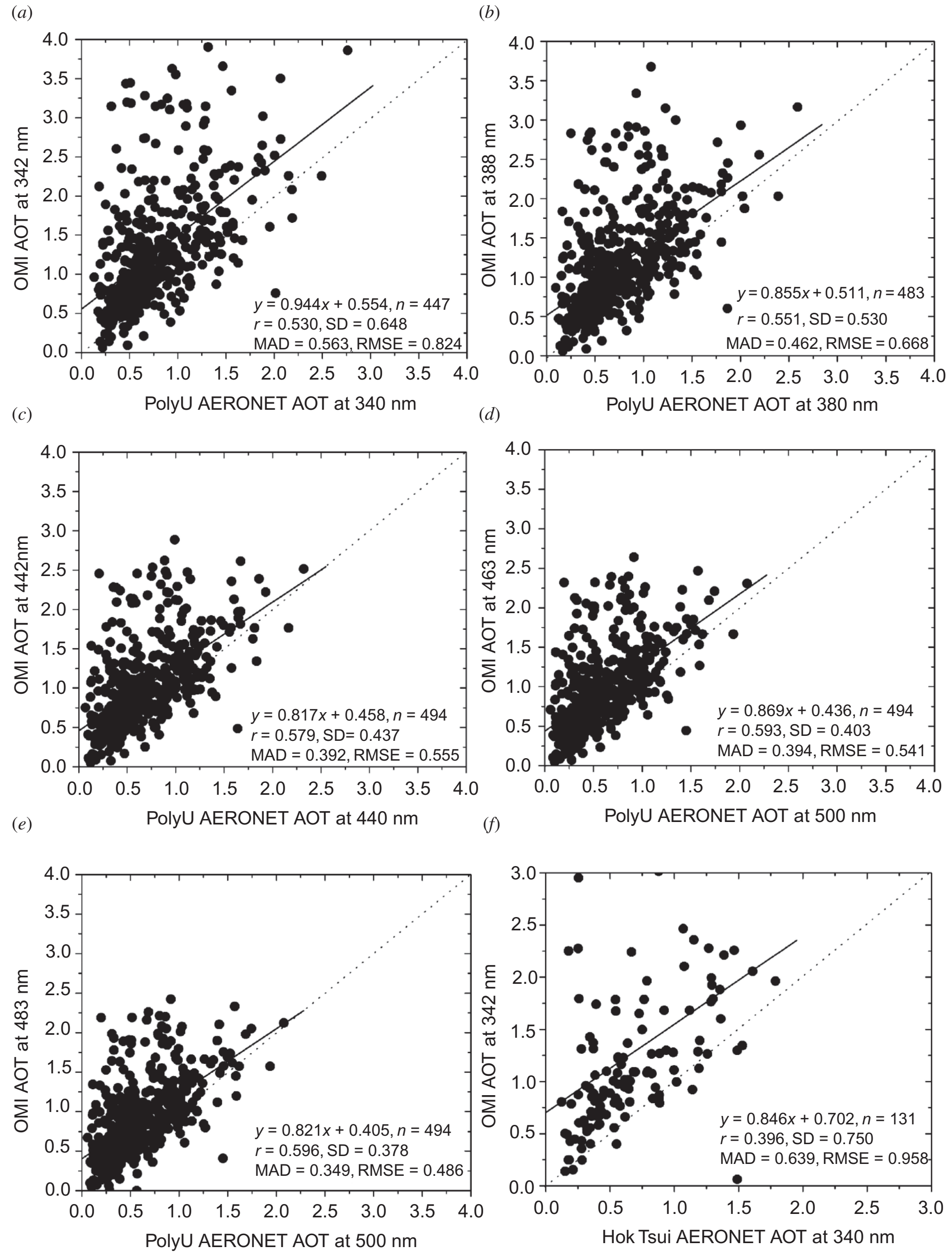

Figure 5. Comparison between OMI 27.8 km AOT and Hong Kong PolyU AERONET data at (*a*) 340 nm, (*b*) 380 nm, (*c*) 442 nm, (*d*) 463 nm, and (*e*) 483 nm, Hong Kong Hok Tsui AERONET data at (*f*) 340 nm, (*g*) 380 nm, (*h*) 442 nm, (*i*) 463 nm, and (*j*) 483 nm, and CityU sunphotometer data at (*k*) 442 nm, (*l*) 463 nm, and (*m*) 483 nm.

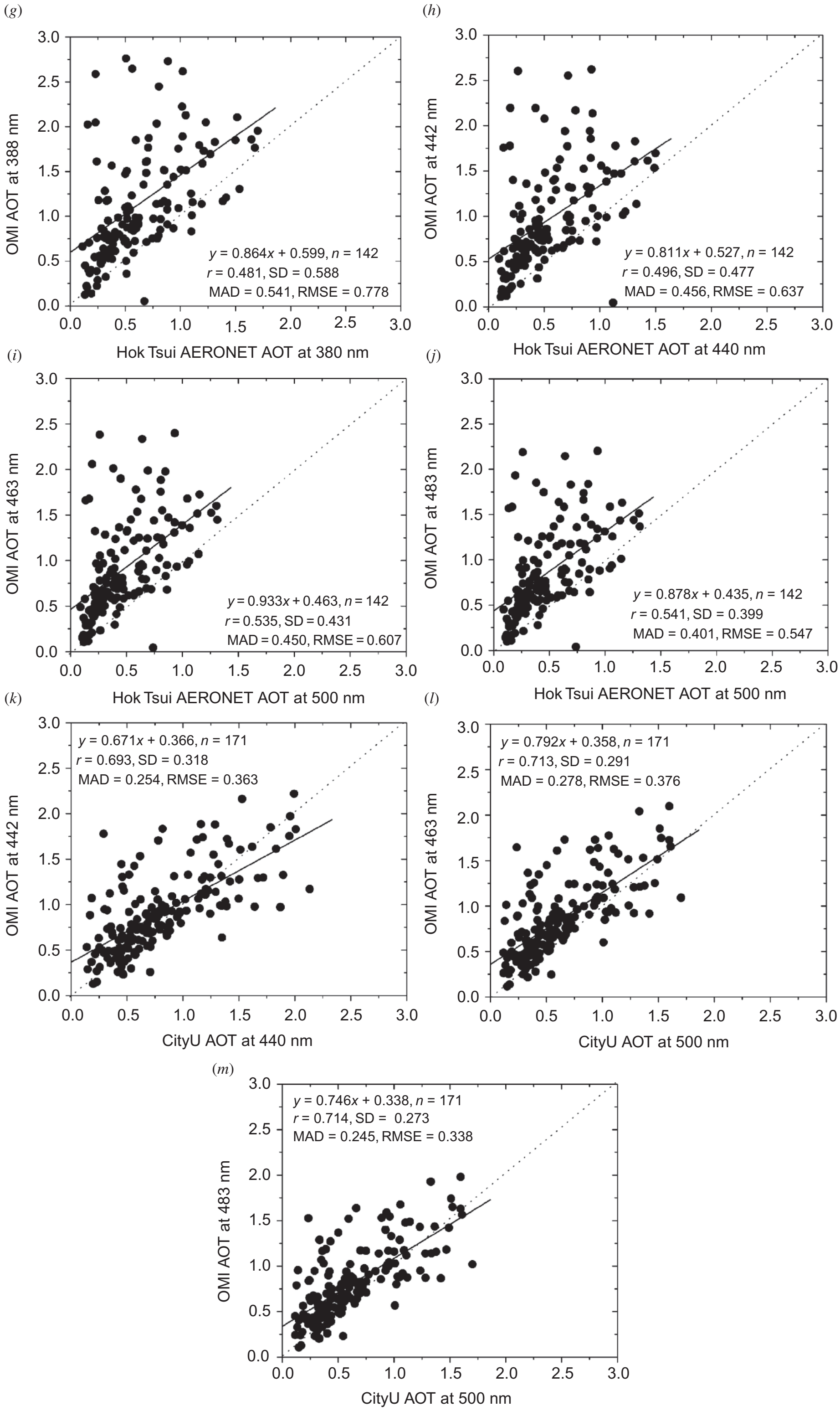

Figure 5. (*Continued*).

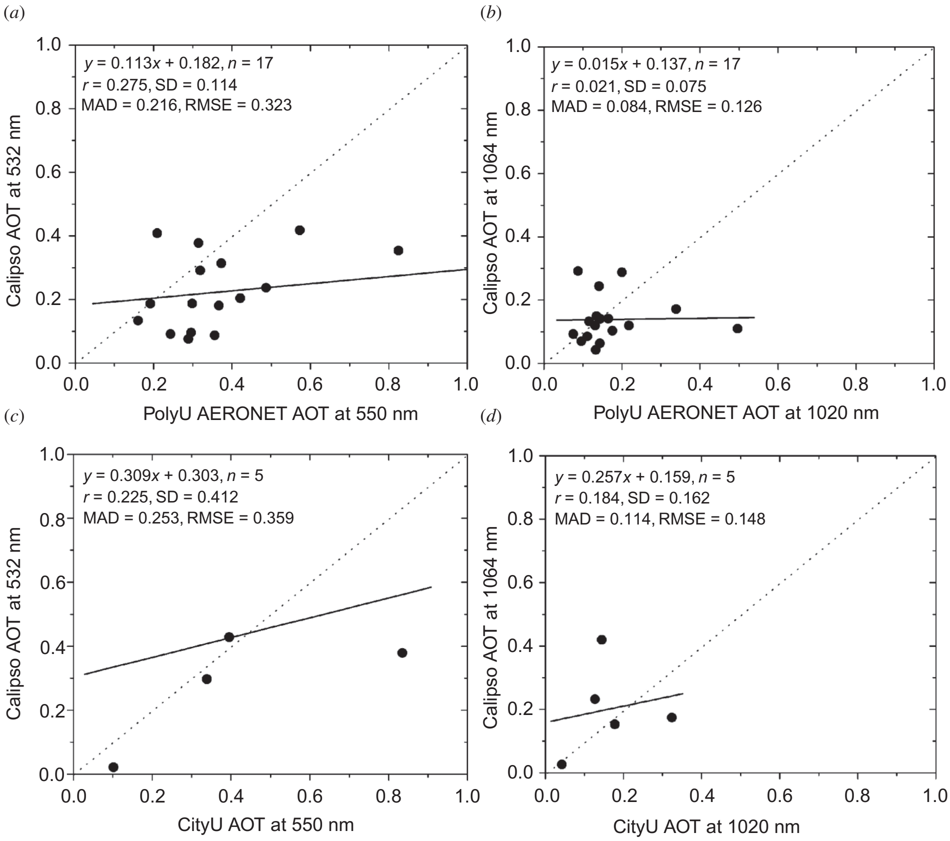

Figure 6. Comparison between CALIPSO 5 km AOT and Hong Kong PolyU AERONET data at (*a*) 550 nm and (*b*) 1020 nm, and CityU sunphotometer data at (*c*) 550 nm and (*d*) 1020 nm.

5. Analysis of the MODIS 10 km AOT data

Since understanding the temporal and spatial patterns of pollutants in terms of the relative contribution of seasonal variations, meteorological parameters, and particle sizes is critical in the reliable prediction of AOT, a few more specific studies have been conducted to examine these independent variables. The MODIS 10 km AOT data with the maximum absolute and relative accuracies are used in this section.

5.1. *Accuracy of MODIS 10 km AOT data (seasonal variation)*

The seasonal patterns of meteorological data were studied to understand their influence on AOT derivation during four seasons. The paired data sets for MODIS 10 km and the three sunphotometers' AOT were grouped by season, namely spring (March–May), summer (June–August), autumn (September–November), and winter (December–February). The results show marked seasonal influence (Table 1). The relative accuracies (correlation) of AOT are generally higher in winter and spring than in summer and autumn, and the results for all sites and seasons are significant at the 1% confidence interval. This may be due to the high atmospheric water vapour content (high relative humidity), causing aerosol particles to grow in size during the rainy season, which may reduce the retrieval accuracy.

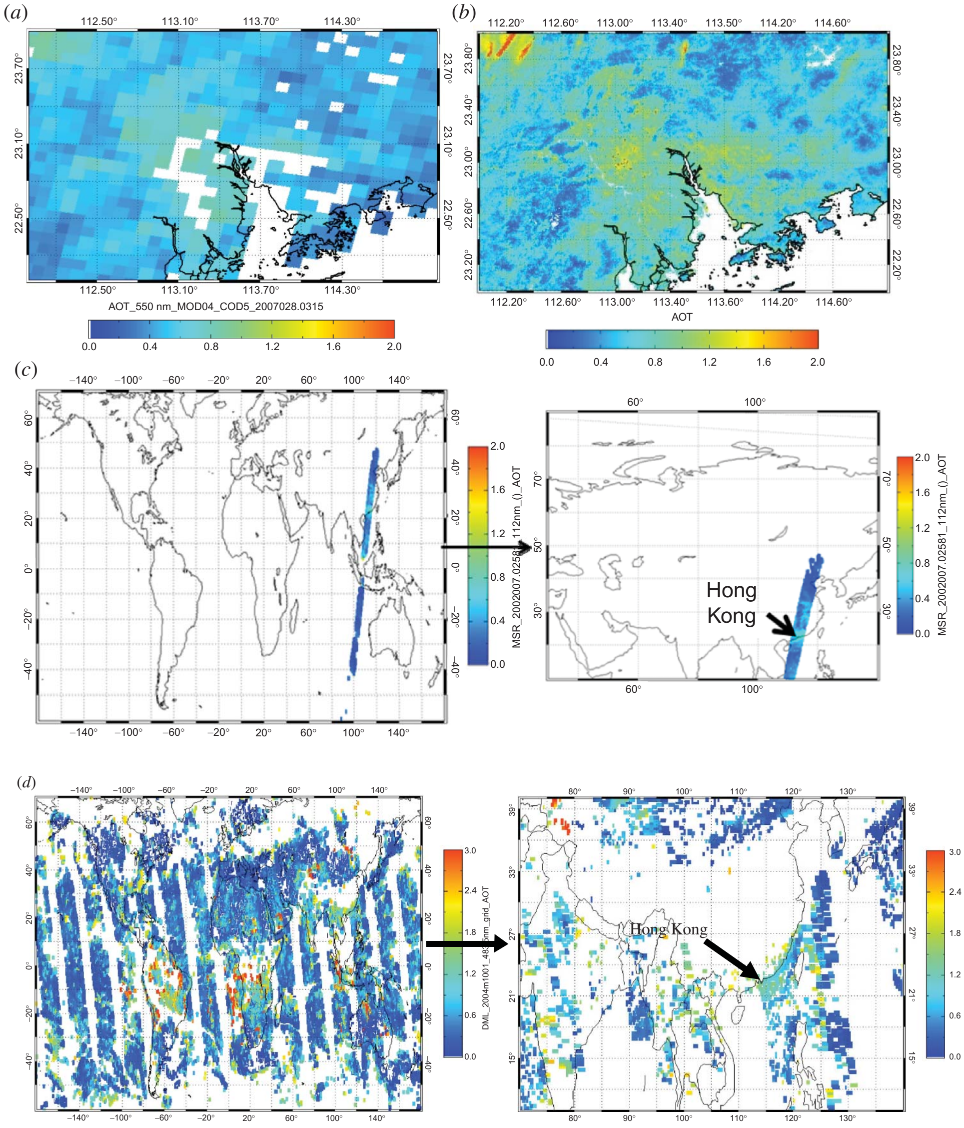

Figure 7. AOT images of (*a*) MODIS 10 km at 550 nm, (*b*) MODIS 500 m at 550 nm, (*c*) MISR at 442 nm, (*d*) OMI at 483 nm, and (*e*) CALIPSO at 532 nm, and (*f*) RGB true colour and MODIS AOT 1 km images. Biomass burning is circled on both images in (*f*).

5.2. Accuracy of MODIS 10 km AOT data (relationship with meteorological parameters)

In order to understand the relationship between AOT and meteorological parameters, the matched data of MODIS 10 km and PolyU AERONET AOT data were categorized according to different weather conditions. Three categories of wind speed (0–2, 2.1–4, and >4.1 m s^{-1}), four categories of wind direction (0–90°, 91–180°, 181–270°, and 270–359°), and five categories of relative humidity (31–40%, 41–50%, 51–60%, 61–70%, and 71–80%) were set, and these data were selected within ±30 min of meteorological

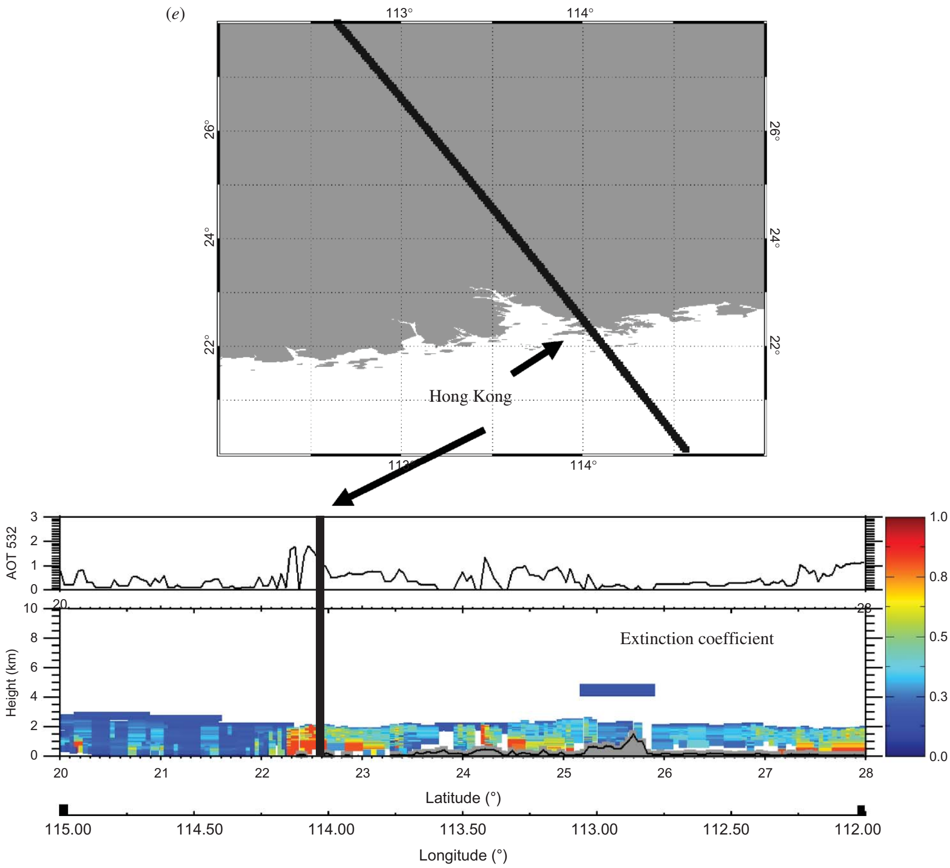

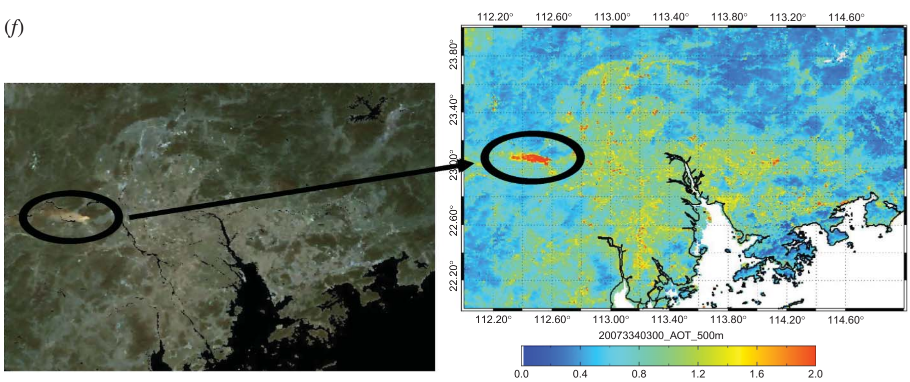

Figure 7. (*Continued*).

observations. The absolute and relative accuracies are shown in Table 2. All the relative accuracies are significant at the 1% confidence interval except on occasions when relative humidity is between 31% and 40%. In addition, high absolute errors are observed when relative humidity is between 71% and 80% and wind direction is between 271° and 359°.

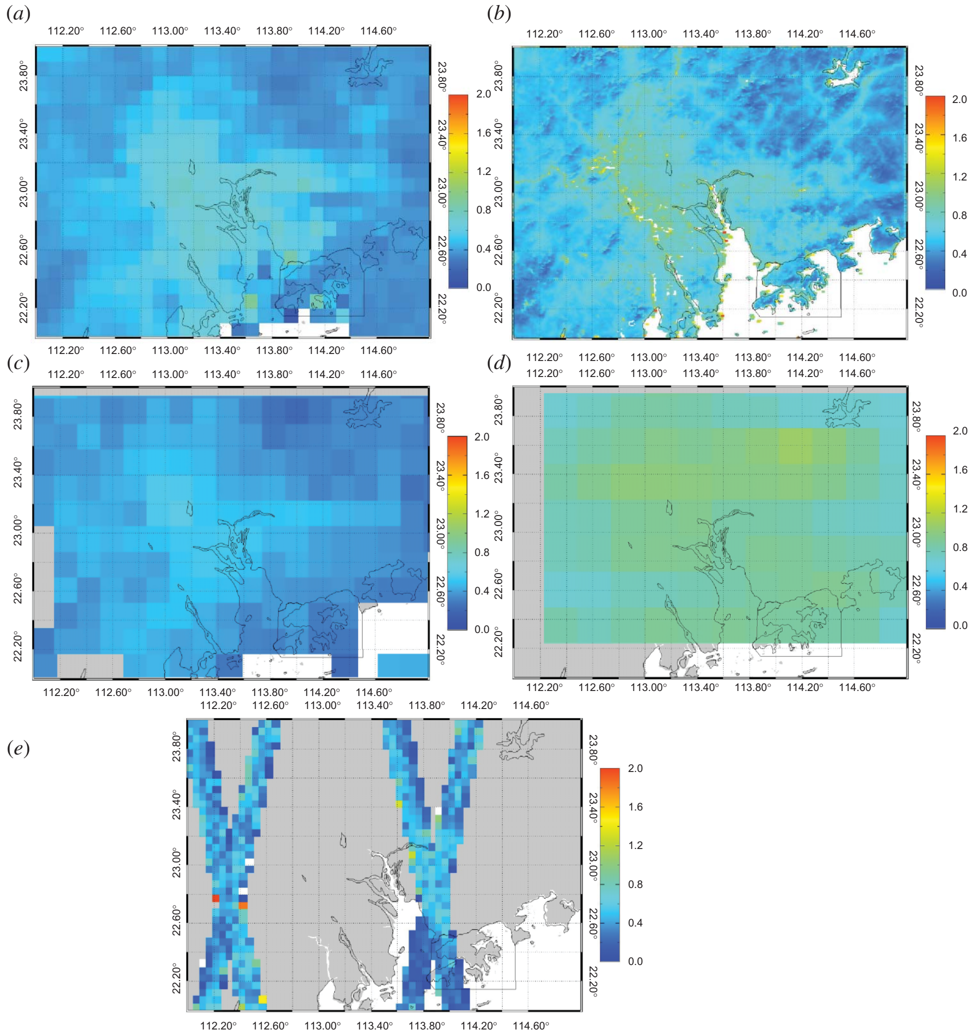

Figure 8. Averaged images of (*a*) MODIS 10 km AOT at 550 nm from 2000 to 2010, (*b*) MODIS 500 m AOT at 550 nm from 2000 to 2011, (*c*) MISR 17.6 km AOT at 558 nm from 2005 to 2010, (*d*) OMI 27.8 km AOT at 483 nm from 2004 to 2010, and (*e*) CALIPSO 5 km AOT at 532 nm from 2006 to 2010.

Table 1. Correlations of MODIS 10 km AOT and sunphotometer data categorized by seasons.

Site/season	Winter	Spring	Summer	Autumn
PolyU AERONET	0.943 (0.128)	0.958 (0.154)	Not enough data	0.937 (0.124)
Hok Tsui AERONET	0.946 (0.084)	Not enough data	Not enough data	Not enough data
CityU sunphotometer	0.930 (0.193)	0.982 (0.139)	0.932 (0.141)	0.954 (0.148)

Note: Values in brackets are root mean square errors.

Table 2. Correlations and root mean square errors of MODIS 10 km AOT and PolyU AERONET data categorized by different meteorological factors.

Meteorological parameters	WD (0–90)	WD (91–180)	WD (181–270)	WD (271–359)	WS (0–2)	WS (2.1–4)	WS (>4.1)	RH (31–40)	RH (41–50)	RH (51–60)	RH (61–70)	RH (71–80)
Correlation	0.951	0.933	*	0.992	0.978	0.937	0.913	0.772	0.981	0.933	0.918	0.982
RMSE	0.119	0.151	*	0.303	0.172	0.130	0.145	0.073	0.128	0.105	0.137	0.272

Notes: *Not enough data. WD represents wind direction (in degrees); WS represents wind speed (in m s^{-1}); RH represents relative humidity (in %).

5.3. *Accuracy of MODIS 10 km AOT data (relationship with particle sizes)*

AERONET contains data of both fine and coarse mode optical thickness based on a spectral deconvolution method (O'Neill, Dubovik, and Eck 2001; O'Neill et al. 2003). MODIS also provides products with the total aerosol optical concentration and the fraction of the optical thickness contributed by the fine and coarse aerosols (Remer et al. 2002). The MODIS fine and coarse mode AOTs (at 550 nm) were acquired and matched with the fine and coarse mode AOTs (at 500 nm) from PolyU and Hok Tsui AERONET sites within ±30 min of overpass time. Table 3 shows the absolute (RMSE) and relative (correlation) accuracies. All the absolute accuracies show moderate to low RMSE for both fine and coarse mode AOTs. The relative accuracies of fine mode AOTs compared with PolyU and Hok Tsui AERONETs are significant at the 1% confidence interval. However, low correlations are observed for the coarse mode AOTs. Similar accuracy is observed for fine mode AOT over the ocean ($r = 0.728$) in Kleidman et al.'s (2005) study but no literature has reported the accuracy of coarse mode AOT over land. These low accuracies observed at coarse mode over land may be due to the longer wavelengths used in MODIS, which estimates fine mode fraction more effectively than coarse mode fraction (Tanré, Herman, and Kaufman 1996; Kleidman et al. 2005). In addition, the MODIS inversion is based on LUTs consisting of four fine modes and five coarse modes, for which the aerosol optical library is smaller than that in AERONET. Thus a large discrepancy in coarse mode AOT is obtained.

6. Discussion and conclusion

The accuracy of aerosol retrieval is mainly dependent on the derivation of surface reflectance and the fit of the aerosol model. In this study, five AOT products (MODIS 10 km, MODIS 500 m, MISR, OMI, and CALIPSO) were validated by comparison with three sunphotometers in Hong Kong. The strongest correlations were obtained from the MODIS 10 km product for all three sunphotometer stations, PolyU AERONET, Hok Tsui AERONET, and CityU, with an average correlation of $r = 0.947$ (Table 4).

Table 5 shows the absolute accuracy assessments (standard deviation (SD), MAD, and RMSE) for different sensors. The findings are in line with the correlations (relative

Table 3. Correlations and root mean square errors (in brackets) categorized by fine and coarse mode AOTs.

Site/mode of AOT	Fine mode	Coarse mode
PolyU AERONET	0.836 (0.281)	0.357 (0.124)
Hok Tsui AERONET	0.889 (0.160)	0.270 (0.092)

Table 4. Relative accuracy of five different sensors.

Satellite	Resolution	Maximum correlation	Minimum correlation	Average correlation	Best/least application
MODIS 10 km	10 km	0.950	0.944	0.947	Urban/coastal
MODIS 500 m	500 m	0.931	0.856	0.886	Coastal/suburban
MISR	17.6 km	0.896	0.818	0.857	Urban/suburban
OMI	27.8 km	0.707	0.490	0.589	Suburban/coastal
CALIPSO	5 km	0.205	0.148	0.176	Suburban/urban

Table 5. Absolute accuracy of five different sensors (the values are averaged from all sites and all wavelengths).

Satellite	Standard deviation	Mean absolute difference	Root mean square error
MODIS 10 km	0.082	0.096	0.123
MODIS 500 m	0.137	0.117	0.138
MISR	0.081	0.188	0.239
OMI	0.456	0.417	0.591
CALIPSO	0.191	0.167	0.239

accuracy assessment) showing that MODIS 10 km data perform well with lower errors (SD = 0.082, MAD = 0.096, RMSE = 0.123).

Difference in accuracy may often be attributed to different signal-to-noise ratios at different resolutions, but in this study, no significant trend in accuracy was observed with either increasing or decreasing resolution (Figure 9(*a*)). The AOT differences due to signal-to-noise ratios may be small, or are small enough to be compensated by the other errors such as the mixed pixel problem, surface reflectance, and the aerosol models used. For example, the higher accuracy observed with MODIS 10 km data (Figure 9(*b*)) than with the MODIS 500 m product is attributed to the higher signal-to-noise ratio obtained with lower resolution, which compensates for the problem of mixed pixels in the surface reflectance estimation. The same explanation can be given for the MISR 17.6 km resolution product, along with MISR's better selection of aerosol models. The somewhat lower accuracy for the higher resolution 500 m product from MODIS may suffer from a lower signal-to-noise ratio but this is partially offset by better surface reflectance estimation from fewer mixed pixels. However, the MODIS 500 m AOT image is capable of identifying discrete pollution sources such as biomass burning plumes (Figure 7(*f*)), which are not resolvable on the other lower resolution AOT products.

A study of MODIS 10 km AOT data was also conducted to examine the influence of seasonal variation, meteorological parameters, and particle sizes on retrieval accuracies. The results suggest that higher accuracy can be obtained during dry seasons and in non-windy and non-humid environments. Since the accuracy of aerosol retrieval is highly dependent on aerosol models in the LUT, the large particle size from sea salts and high water vapour contents may not be accounted for in the standard MODIS LUTs.

Overall, this study indicates that the highest performance can be obtained from MODIS 10 km products (Figure 9) especially during non-humid days and when fine (submicron) aerosols dominate. These AOT products can provide reliable and accurate observations for daily air monitoring, as well as for identifying emission sources for coordinated actions by the Hong Kong and Guangdong governments to tackle regional pollution. However, the depiction of more local patterns of air quality on an intra-urban scale, represented by the MODIS 500 m AOT product, suffers from a somewhat lower accuracy and requires further refinement of the retrieval algorithm.

Acknowledgements

The authors would like to acknowledge the NASA Goddard Earth Sciences Distributed Active Archive Center for the MODIS level IB and level 2 data, MISR products, and OMI data, and the City University of Hong Kong for sunphotometer data. The CALIPSO data were obtained from the NASA Langley Research Center Atmospheric Science Data Center. Grants PolyU 5253/10E and B-Q23L from the Hong Kong RGC and Grant ECF 33/2010 from the Hong Kong Environment and Conservation Fund sponsored the research. K.H. Lee's work was funded by the Korea Meteorological Administration Research and Development Programme under Grant CATER 2012-7080.

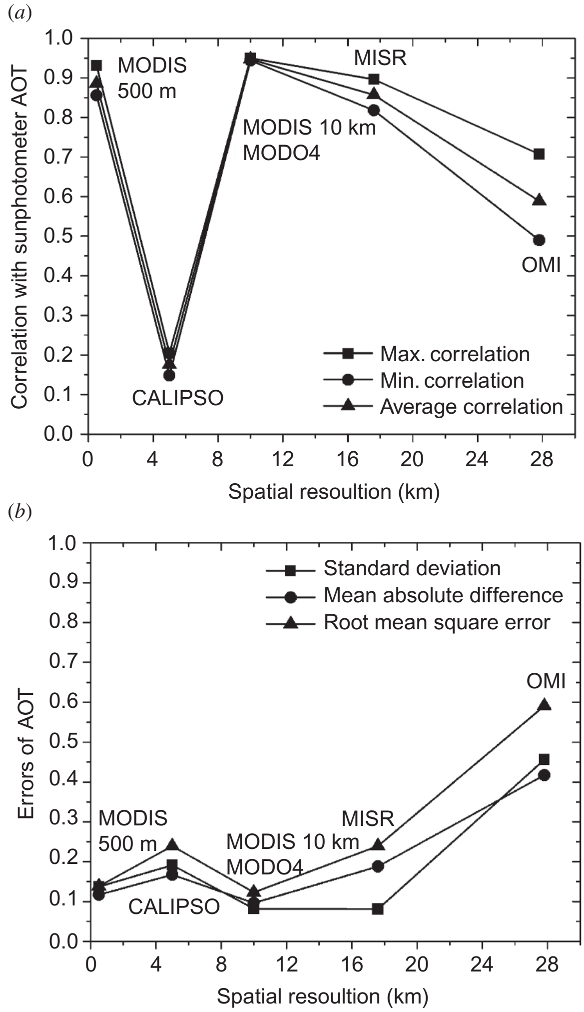

Figure 9. (*a*) Maximum, minimum, and average correlations for the five different AOT products and (*b*) standard deviations, mean absolute differences, and root mean square errors for the five different AOT products.

References

Bell, G. J., P. Peterson, and P. C. Chin. 1970. "*Meteorological Aspects of Atmospheric Pollution in Hong Kong*." Royal Observatory Technical Note No. 29.

Bhartia, P. K., and C. W. Wellemeyer. 2002. "OMI TOMS-V8 Total O3 Algorithm." In *Algorithm Theoretical Baseline Document: OMI Ozone Products*, edited by P. K. Bhartia, Vol. II, ATBD-OMI-02, Version 2.0. Greenbelt, MD: NASA Goddard Space Flight Center. Accessed December 19, 2011. http://eospso.gsfc.nasa.gov/eos_homepage/for_scientists/atbd/docs/Omi/Atbd-Omi-02.pdf.

Bovensmann, H., J. P. Burrows, M. Buchwitz, J. Frerick, S. Noel, V. V. Rozanov, K. V. Chance, and A. P. H. Goede. 1999. "SCIAMACHY: Mission Objectives and Measurement Modes." *Journal of the Atmospheric Sciences* 56: 127–50.

Burrows, J. P., E. Hölzle, A. P. H. Goede, H. Visser, and W. Fricke. 1995. "SCIAMACHY: Scanning Imaging Absorption Spectrometer for Atmospheric Cartography." *Acta Astronautica* 35: 445–51.

Burrows, J. P., M. Weber, M. Buchwitz, V. Rozanov, A. Ladstatter-Weissenmayer, A. Richter, R. De Beek, R. Hoogen, K. Bramstedt, W. Eichmann, M. Eisinger, and D. Perner. 1999. "The Global Ozone Monitoring Experiment (GOME): Mission Concept and First Scientific Results." *Journal of Atmospheric Sciences* 56: 151–75.

Chang, W. L., and E. H. Koo. 1986. "A Study of Visibility Trends in Hong Kong (1968–1982)." *Atmospheric Environment* 20: 1847–58.

Cheng, Y. S., M. H. Chan, and X. Yang. 2006. "Study of Aerosol Optical Thickness in Hong Kong, Validation, Results, and Dependence on Meteorological Parameters." *Atmospheric Environment* 40: 4469–77.

Curier, R. L., J. P. Veefkind, R. Braak, B. Veihelmann, O. Torres, and G. De Leeuw. 2008. "Retrieval of Aerosol Optical Properties from OMI Radiances Using a Multiwavelength Algorithm: Application to Western Europe." *Journal of Geophysical Research* 113: D17S90. doi:10.1029/2007JD008738.

Davidson, C. I., R. F. Phalen, and P. A. Solomon. 2005. "Airborne Particulate Matter and Human Health: A Review." *Aerosol Science and Technology* 39: 737–49.

Diner, D. J., J. C. Beckert, T. H. Reilly, C. J. Bruegge, J. E. Conel, R. A. Kahn, J. V. Martonchik, T. P. Ackerman, R. Davies, S. A. W. Gerstl, H. R. Gordon, J. Muller, R. B. Myneni, P. J. Sellers, B. Pinty, and M. M. Verstraete. 1998. "Multi-Angle Imaging SpectroRadiometer (MISR) Instrument Description and Experiment Overview." *IEEE Transactions on Geoscience and Remote Sensing* 36: 1072–87.

Dobber, M. R., R. Dirksen, P. Levelt, G. H. J. van den Oord, R. Voors, Q. Kleipool, G. Jaross, M. Kowalewski, E. Hilsenrath, G. Leppelmeier, J. de Vries, W. Dierssen, and N. Rozemeijer. 2006. "Ozone Monitoring Instrument Calibration." *IEEE Transactions on Geoscience and Remote Sensing* 44: 1209–38.

Dominici, F., R. D. Peng, M. Bell, L. Pham, D. Mcdermott, J. Zeger, and J. Samet. 2006. "Fine Particulate Air Pollution and Hospital Admission for Cardiovascular and Respiratory Diseases." *The Journal of the American Medical Association* 295: 1127–34.

DRAGON-US. 2011. "NASA's AERONET Field Campaign, Distributed Regional Aerosol Gridded Observation Networks (DRAGON)-USA 2011." Accessed December 19, 2011. http://aeronet.gsfc.nasa.gov/new_web/dragon.html.

Heath, D. F., and H. Park. 1978. "The Solar Backscatter Ultraviolet (SBUV) and Total Ozone Mapping Spectrometer (TOMS) Experiment." In *The Nimbus-7, Users' Guide*, edited by C. R. Madrid, 175 p. Greenbelt, MD: NASA Goddard Space Flight Center.

Hidy, G., J. Brook, J. Chow, M. Green, M. Green, R. Husar, C. Lee, R. Scheffe, A. Swanson, and J. Watson. 2009. "The A&WMA 2009 Critical Review Discussion – Remote Sensing of Particulate Pollution from Space: Have We Reached the Promised Land?" *Journal of the Air & Waste Management Association* 59: 1130–9.

Hobbs, P. V. 1993. *Aerosol–Cloud–Climate Interactions*. San Diego, CA: Academic Press.

Holben, B. N., T. F. Eck, I. Slutsker, D. Tanré, J. P. Buis, A. Setzer, E. F. Vermote, J. A. Reagan, Y. J. Kaufman, T. Nakajima, F. Lavenu, I. Jankowiak, and A. Smirnov. 1998. "AERONET – A Federated Instrument Network and Data Archive for Aerosol Characterization." *Remote Sensing of Environment* 66: 1–16.

Hsu, N. C., S. C. Tsay, and M. D. King. 2006. "Deep Blue Retrievals of Asian Aerosol Properties during ACE-Asia." *IEEE Transactions on Geoscience and Remote Sensing* 44: 3180–95.

Hsu, N. C., S. C. Tsay, M. D. King, and J. R. Herman. 2004. "Aerosol Properties over Bright-Reflecting Source Regions." *IEEE Transactions on Geoscience and Remote Sensing* 42: 557–69.

Ichoku, C., D. A. Chu, S. Mattoo, Y. J. Kaufman, L. A. Remer, D. Tanré, I. Slusker, and B. N. Holben. 2002. "A Spatio-Temporal Approach for Global Validation and Analysis of MODIS Aerosol Products." *Geophysical Research Letter* 29. doi:10.1029/2001GL013206.

Jethva, H., and O. Torres. 2011. "Satellite-Based Evidence of Wavelength-Dependent Aerosol Absorption in Biomass Burning Smoke Inferred from Ozone Monitoring Instrument." *Atmospheric Chemistry and Physics Discussion* 11: 7291–319.

Jiang, X., Y. Liu, B. Yu, and M. Jiang. 2007. "Comparison of MISR Aerosol Optical Thickness with AERONET Measurements in Beijing Metropolitan Area." *Remote Sensing of Environment* 107: 45–53.

Junge, C. E. 1952. "Die Konstitution der Atmospherischen Aerosols." *Annalen* der *Meteorologie*, 1: 128–35.

Kahn, R., P. Banerjee, and D. McDonald. 2001. "Sensitivity of Multiangle Imaging to Natural Mixtures of Aerosols over Ocean." *Journal of Geophysical Research* 106, no. D16: 18219–38.

Kahn, R. A., B. J. Gaitley, J. V. Martonchik, D. J. Diner, K. A. Crean, and B. Holben. 2005. "Multiangle Imaging Spectroradiometer (MISR) Global Aerosol Optical Depth Validation Based on 2 Years of Coincident Aerosol Robotic Network (AERONET) Observations." *Journal of Geophysical Research* 110: D10S04. doi:10.1029/2004JD004706.

Kaufman, Y. J., N. Gobron, B. Pinty, J. L. Widlowski, and M. M. Verstraete. 2002. "Relationship between Surface Reflectance in the Visible and Mid-IR Used in MODIS Aerosol Algorithm – Theory." *Geophysical Research Letters* 29: 2116. doi:10.1029/2001GL014492.

Kaufman, Y. J., and C. Sendra. 1988. "Algorithm for Automatic Atmospheric Corrections to Visible and Near-IR Satellite Imagery." *International Journal of Remote Sensing* 9: 1357–81.

Kaufman, Y. J., and D. Tanré. 1998. Algorithm for remote sensing of tropospheric aerosols from MODIS, MODIS Algorithm Theoretical Basis Document, Product ID: MOD04, Revised 26 October, 1998.

Kaufman, Y. J., D. Tanré, H. R. Gordon, T. Nakajima, J. Lenoble, R. Frouin, H. Grassl, B. M. Herman, M. D. King, and P. M. Teillet. 1997. "Passive Remote Sensing of Tropospheric Aerosol and Atmospheric Correction for the Aerosol Effect." *Journal of Geophysical Research* 102, no. D14: 16815–30.

King, M. D., Y. J. Kaufman, D. Tanré, and T. Nakajima. 1999. "Remote Sensing of Tropospheric Aerosols from Space: Past, Present, and Future." *Bulletin of the American Meteorological Society* 80: 2229–59.

King, M. D., S. Platnick, P. Yang, G. T. Arnold, M. A. Gray, J. C. Riedi, S. A. Ackerman, and K. N. Liou. 2004. "Remote Sensing of Liquid Water and Ice Cloud Optical Thickness and Effective Radius in the Arctic: Application of Airborne Multispectral MAS Data." *Journal of Atmospheric and Oceanic Technology* 21: 857–75.

Kleidman, R. G., N. T. O'Neill, L. A. Remer, Y. J. Kaufman, T. F. Eck, D. Tanré, O. Dubovik, and B. N. Holben. 2005. "Comparison of Moderate Resolution Imaging Spectroradiometer (MODIS) and Aerosol Robotic Network (AERONET) Remote-Sensing Retrievals of Aerosol Fine Mode Fraction over Ocean." *Journal of Geophysical Research* 110: D22205. doi:10.1029/2005JD005760.

Kokhanovsky, A., F. Breon, A. Cacciari, E. Carboni, D. Diner, W. Dinicolantonio, R. Grainger, W. Grey, R. Holler, and K. Lee. 2007. "Aerosol Remote Sensing over Land: A Comparison of Satellite Retrievals Using Different Algorithms and Instruments." *Atmospheric Research* 85: 372–94.

Lai, L. Y., and R. Sequeira. 2001. "Visibility Degradation across Hong Kong: Its Components and Their Relative Contributions." *Atmospheric Environment* 35: 5861–72.

Lee, K. H., K. Y. Joon, W. Von Hoyningen-Huene, and J. Burrow. 2006. "Influence of Land Surface Effects on MODIS Aerosol Retrieval Using the BAER Method over Korea." *International Journal of Remote Sensing* 27: 2813–30.

Lee, K. H., and Y. J. Kim. 2010. "Satellite Remote Sensing of Asian Aerosols: A Case Study of Clean, Polluted and Dust Storm Days." *Atmospheric Measurement Techniques* 3: 2651–80.

Lee, K. H., Z. Li, Y. J. Kim, and A. Kokhanovsky. 2009. "Atmospheric Aerosol Monitoring from Satellite Observations: A History of Three Decades." In *Atmospheric and Biological Environmental Monitoring*, edited by Y. J. Kim, U. Platt, M. B. Gu, and H. Iwahashi, 13–38. The Netherlands: Springer. ISBN 978-1-4020-9673–0.

Levelt, P. F., E. Hilsenrath, G. W. Leppelmeier, G. H. J. Van Den Oord, P. K. Bhartia, J. Tamminen, J. F. De Haan, and J. P. Veefkind. 2006. "Science Objectives of the Ozone Monitoring Instrument." *IEEE Transactions on Geoscience and Remote Sensing* 44: 1199–1208.

Levy, R. C., L. A. Remer, J. V. Martins, Y. J. Kaufman, A. Plana-Fattori, J. Redemann, and B. Wenny. 2005. "Evaluation of the MODIS Aerosol Retrievals over Ocean and Land during CLAMS." *Journal of the Atmospheric Sciences* 62: 974–92.

Liu, J., X. Xia, Z. Li, P. Wang, M. Min, W. O. Ha, Y. Wang, J. Xin, X. Li, Y. Zheng, and Z. Chen. 2010. "Validation of Multi-Angle Imaging Spectroradiometer Aerosol Products in China." *Tellus Series B, Chemical and Physical Meteorology* 62: 117–24.

Martonchik, J. V., D. J. Diner, R. A. Kahn, T. P. Ackerman, M. M. Verstraete, B. Pinty, and H. R. J. Gordon. 1998. "Techniques for the Retrieval of Aerosol Properties over Land and Ocean Using Multiangle Imaging." *IEEE Transactions on Geoscience and Remote Sensing* 36: 1212–27.

Mie, G. 1908. "On Optical Characteristics of Turbid Media, with Special Reference to Colloid Metallic Solutions." *Annals of Physics* 25: 377–445.

O'Neill, N. T., O. Dubovik, and T. F. Eck. 2001. "A Modified Angstrom Coefficient for the Characterization of Sub-Micron Aerosols." *Applied Optics* 40: 2368–74.

O'Neill, N. T., T. F. Eck, A. Smirnov, B. N. Holben, and S. Thulasiraman. 2003. "Spectral Discrimination of Coarse and Fine Mode Optical Depth." *Journal of Geophysical Research* 108, no. D17: 4559. doi:10.1029/2002JD002975.

Parkinson, C. L. 2003. "Aqua: An Earth-Observing Satellite Mission to Examine Water and Other Climate Variables." *IEEE Transactions on Geoscience and Remote Sensing* 41: 173–83.

Remer, L. A., Y. J. Kaufman, D. Tanré, S. Mattoo, D. A. Chu, J. V. Martins, R.-R. Li, C. Ichoku, R. C. Levy, R. G. Kleidman, T. F. Eck, E. Vermote, and B. N. Holben. 2005. "The MODIS Aerosol Algorithm, Products and Validation." *Journal of the Atmospheric Science* 62: 947–73.

Remer, L. A., D. Tanré, Y. J. Kaufman, C. Ichoku, S. Mattoo, R. Levy, D. A. Chu, B. Holben, O. Dubovik, A. Smirnov, J. V. Martins, R. R. Li, and Z. Ahmad. 2002. "Validation of MODIS Aerosol Retrieval over Ocean." *Geophysical Research Letters* 29: 4.

Smirnov, A., B. N. Holben, T. F. Eck, O. Dubovik, and I. Slutsker. 2000. "Cloud-Screening and Quality Control Algorithms for the AERONET Database." *Remote Sensing of Environment* 73: 337–49.

Tanré, D., M. Herman, and Y. J. Kaufman. 1996. "Information on Aerosol Size Distribution Contained in Solar Reflected Spectral Radiances." *Journal of Geophysical Research* 101: 19043–60.

Torres, O., P. K. Bhartia, J. R. Herman, Z. Ahmad, and J. Gleason. 1998. "Derivation of Aerosol Properties from Satellite Measurements of Backscattered Ultraviolet Radiation: Theoretical Basis." *Journal of Geophysical Research* 103, no. D14: 17099–110.

Torres, O., P. K. Bhartia, A. Sinyuk, E. J. Welton, and B. Holben. 2005. "Total Ozone Mapping Spectrometer Measurements of Aerosol Absorption from Space: Comparison to SAFARI 2000 Ground-Based Observations." *Journal of Geophysical Research* 110: D10S18. doi:10.1029/2004JD004611.

Von Hoyningen-Huene, W., A. A. Kokhanovsky, M. W. Wuttke, M. Buchwitz, S. Noël, K. Gerilowski, J. P. Burrows, B. Latter, R. Siddans, and B. J. Kerridge. 2006. "Validation of SCIAMACHY Top-of-Atmosphere Reflectance for Aerosol Remote Sensing Using MERIS L1 Data." *Atmospheric Chemistry and Physics* 7: 97–106.

Winker, D. M., W. H. Hunt, and M. J. Mcgill. 2007. "Initial Performance Assessment of CALIOP." *Geophysical Research Letters* 34: L19803. doi:10.1029/2007GL030135.

Winker, D. M., J. Pelon, J. A. Coakley, S. A. Ackerman, R. J. Charlson, P. R. Colarco, P. Flamant, Q. Fu, R. M. Hoff, C. Kittaka, T. L. Kubar, H. L. Treut, M. P. McCormick, G. Mégie, L. Poole, K. Powell, C. Trepte, M. A. Vaughan, and B. A. Wielicki. 2010. "The CALIPSO Mission: A Global 3D View of Aerosols and Clouds." *Bulletin of the American Meteorological Society* 91: 1211–29.

Winker, D. M., J. R. Pelon, and M. P. Mccormick. 2003. "The CALIPSO Mission: Space Borne Lidar for Observation of Aerosols and Clouds, in Lidar Remote Sensing for Industry and Environment Monitoring III." In *Proceedings of the Meeting, SPIE*, edited by U. N. Singh, T. Itabe, and Z. Liu, Vol. 4893, 1–11. Bellingham, WA: SPIE EurOpto Series.

Wong, M. S., J. E. Nichol, and K. H. Lee. 2011. "An Operational MODIS Aerosol Retrieval Algorithm at High Spatial Resolution, and Its Application over a Complex Urban Region." *Atmospheric Research* 99: 570–89.

Wong, M. S., J. E. Nichol, K. H. Lee, and Z. Li. 2010. "Retrieval of Aerosol Optical Thickness Using MODIS 500 $\times$ 500 m^2, a Study in Hong Kong and Pearl River Delta Region." *IEEE Transactions on Geoscience and Remote Sensing* 48: 3318–27.